

D. M. Koh  
G. Brown  
A. M. Riddell  
E. Scurr  
D. J. Collins  
S. D. Allen  
I. Chau  
D. Cunningham  
N. M. deSouza  
M. O. Leach  
J. E. Husband

## Detection of colorectal hepatic metastases using MnDPDP MR imaging and diffusion-weighted imaging (DWI) alone and in combination

Received: 13 August 2007  
Revised: 16 November 2007  
Accepted: 17 December 2007  
Published online: 12 January 2008  
© European Society of Radiology 2007

D. M. Koh · D. J. Collins ·  
N. M. deSouza · M. O. Leach  
Cancer Research UK Clinical Magnetic  
Resonance Research Group,  
Institute of Cancer Research,  
Sutton, UK

D. M. Koh (✉) · G. Brown ·  
A. M. Riddell · E. Scurr ·  
S. D. Allen · J. E. Husband  
Academic Department of Radiology,  
Royal Marsden Hospital,  
Sutton, UK  
e-mail: dowmukoh@icr.ac.uk  
Tel.: +44-0208-661-3340

I. Chau · D. Cunningham  
Department of Medical Oncology,  
Royal Marsden Hospital,  
Sutton, UK

**Abstract** To compare the diagnostic accuracy of MnDPDP MR imaging and diffusion-weighted imaging (DWI), alone and in combination, for detecting colorectal liver metastases in patients with suspected metastatic disease. Thirty-three consecutive patients with suspected colorectal liver metastases underwent MR imaging. Three image sets (MnDPDP, DWI and combined MnDPDP and DWI) were reviewed independently by two observers. Lesions were scored on a five-point scale for malignancy and the areas ( $A_z$ ) under the receiver operating characteristic curves were calculated for each observer and image set. The sensitivity and specificity for lesion detection were calculated for each image set and compared. There were 83 metastases, 49 cysts and 1 haemangioma. Using the combined

set resulted in the highest diagnostic accuracy for both observers ( $A_z=0.94$  and  $0.96$ ), with improved averaged sensitivity of lesion detection compared with the DWI set ( $p=0.01$ ), and a trend towards improved sensitivity compared with the MnDPDP set ( $p=0.06$ ). There was no difference in the averaged specificity using any of the three image sets ( $p>0.5$ ). Combination of MnDPDP MR imaging and DWI resulted in the highest diagnostic accuracy and can increase sensitivity without loss in specificity.

**Keywords** Liver · Metastases · Diffusion-weighted imaging · MR imaging · Colorectal

### Introduction

In patients with colorectal hepatic metastases, surgical resection can improve survival [1–3]. Patients with liver metastases that can be completely resected have a better 5-year survival rate compared with those with irresectable disease [4]. Using pre-operative chemotherapy, it is possible to downsize and downstage liver disease to render irresectable disease resectable [5]. Hence, accurate detection and localization of metastases before and after pre-operative chemotherapy can help to identify patients who are most likely to benefit from surgery.

The detection of colorectal hepatic metastases can potentially be improved using novel contrast media and new imaging techniques. Mangafodipir trisodium (MnDPDP), a

liver-specific MR contrast agent administered by intravenous contrast infusion, demonstrates colorectal hepatic metastases as hypointense lesions against the avidly enhancing hepatic parenchyma on T1-weighted imaging. Metastases may also demonstrate rim and segmental enhancement at 24 h after MnDPDP contrast administration, which further facilitates their detection [6]. A 90% detection rate for metastases is reported with MnDPDP MR imaging compared with 72% for unenhanced MR imaging and 71% for contrast-enhanced CT [7].

Diffusion-weighted MRI (DWI) is sensitive to the molecular diffusion of water in biologic tissues, and recent advancements have enabled high quality DWI images of the liver to be obtained. Colorectal hepatic metastases show high signal restricted diffusion on DWI compared with

normal liver parenchyma. Using breath-hold single shot echo-planar (EPI) DWI with parallel imaging, Nasu et al. found that DWI had a higher sensitivity and diagnostic accuracy for detecting colorectal hepatic metastases compared with SPIO-enhanced MR imaging [8]. However, the utility and diagnostic accuracy of DWI for the detection of colorectal liver metastases has not been widely reported. Furthermore, the additional value of DWI to contrast-enhanced MR imaging is unknown.

Hence, the purpose of our study was to compare the diagnostic accuracy of MnDPDP MR imaging, diffusion-weighted imaging (DWI) and the combination of MnDPDP MR imaging and DWI for the detection of colorectal hepatic metastases.

## Methods and materials

The study was approved by the institution research review board and ethics committee. Written consent was obtained from patients prior to inclusion in the study.

### Study population

Thirty-eight consecutive patients with liver metastases from colorectal cancer were prospectively evaluated. Patient inclusion criteria were: (1) pathologically proven adenocarcinoma of the colon or rectum, (2) at least one liver lesion detected at CT or ultrasound imaging that was diagnostic or suspicious of liver metastasis and (3) patients were potential candidates for surgical liver resection (i.e. disease sparing of at least two contiguous liver segments). The exclusion criteria were patients with contraindications to MR imaging or prior history of other malignancies, but none were excluded on this basis. In five patients, no evidence of metastatic disease was diagnosed at MR imaging and at follow-up imaging, and they were thus excluded from analysis. Hence, the final study population comprised 33 patients (23 males, 10 females), with a mean age of 57 years (range 45 to 67 years).

### MR technique

MR examinations were performed using a 1.5-T MR system (Gyrosan Intera, Philips Medical Systems, Best, The Netherlands) employing a SENSE body coil.

Unenhanced T1-weighted (gradient echo, TR=128 ms, TE=4.6 ms, 450-cm FOV, 256×256 matrix, SENSE factor 1.8, section thickness 7 mm) and T2-weighted (TR=1,800 ms, TE=40 and 350 ms,  $\alpha=90^\circ$ , 450-mm FOV, 256×256 matrix, SENSE factor 1.8, section thickness 7 mm) axial imaging was performed prior to DWI and MnDPDP contrast administration.

Breath-hold axial single-shot SENSE DWI was performed prior to contrast administration using three gradient factors ( $b=0$ , 150 and 500 s/mm<sup>2</sup>) applied in the frequency select (M), phase select (P) and slice select (S) directions (spin-echo, TR=1,850, TE=56 ms, 340-mm FOV, 112×256 matrix, images re-interpolated to 256×256 matrix, 7-mm thickness, SENSE factor 2). Twelve sections through the liver were acquired in each 20-s breath-hold, and the entire liver (from the level of the diaphragm to the inferior edge of liver) was typically evaluated in two to three breath-holds. Nine images were typically obtained at each level: one  $b=0$  s/mm<sup>2</sup> image, one image in each P, M and S directions at  $b=150$  and 500 s/mm<sup>2</sup>, as well as the trace or index  $b=150$  and 500 s/mm<sup>2</sup> images.

Following intravenous infusion of MnDPDP (0.5 ml/kg body weight administered over 20 min), T1-weighted axial and coronal imaging was performed immediately (typically 20 to 30 min) and at 24 h after contrast administration using the same sequence parameters as the pre-contrast imaging.

### Image interpretation and analysis

Two observers (AR and GB, with 5 and 10 years of experience in abdominal MRI respectively) independently reviewed all images without knowledge of the results of the surgical resection or pathologic analysis. The imaging findings were validated by comparison with histopathology after surgical resection ( $n=17$ ) or follow-up imaging ( $n=16$ ), which were used as gold standards. At follow-up imaging (mean period=8 months; range 6 to 14 months), a lesion was deemed malignant if it showed 20% or greater change in size.

Images were reviewed on a workstation (e-film, Merge Healthcare, Milwaukee, WI) as image sets at three separate readings, with an interval of 1 month between readings. The image sets were as follows:

- (1) *MnDPDP image set*: Unenhanced T1-/T2-weighted images were evaluated with MnDPDP-enhanced MR images.
- (2) *DWI image set*: Unenhanced T1-/T2-weighted images were evaluated with all (trace and direction) DWI images.
- (3) *Combined MnDPDP and DWI image set*: Unenhanced T1-/T2-weighted images were assessed with MnDPDP-enhanced MR and DWI images.

Focal liver lesions identified at review of each image set were assessed by individual observers for:

- (1) *Lesion site*. The location of each lesion was recorded. An anatomic description and slice position of each lesion was also noted to facilitate subsequent lesion matching and comparison.

- (2) *Lesion size.* The largest axial diameter of each lesion was measured in centimetres.
- (3) *Lesion characteristics.* A lesion was deemed metastatic if it showed low T1 signal intensity, variable high T2 signal intensity, as well as rim enhancement/peripheral segmental liver enhancement at MnDPDP MR imaging or high signal intensity on the  $b=500 \text{ s/mm}^2$  DWI images (Fig. 1). The likelihood that a lesion represented a metastasis was scored by each observer on a 5-point scale: 1-definitely not a metastasis; 2-probably not a metastasis; 3-may or may not be a metastasis; 4-probably a metastasis and 5-definitely a metastasis. Receiver operating characteristic curves (ROCs) were constructed based on observer's scoring of lesions using each imaging set and the area under the curves ( $A_z$ ) calculated. When imaging-detected lesions were compared with the gold standard tests, lesions that were confirmed on the reference standards but not visible on MnDPDP MR imaging or DWI were categorised as 'not seen' and classified as 'definitely not a metastasis' (score=1) for the purpose of ROC analysis.

All available imaging and pathologic findings were independently re-reviewed by a radiologist (DMK) to evaluate and record the possible reasons why metastases were missed or misclassified by either observer compared with the reference standard.

#### Statistical analysis

Statistical analysis was performed using MedCalc (MedCalc Inc, Merienke, The Netherlands). Agreement in lesion scoring at imaging was determined using kappa statistics. Kappa values of  $<0.20$  indicate poor agreement,  $0.21\text{--}0.40$  slight agreement,  $0.41\text{--}0.60$  moderate agreement,  $0.61\text{--}0.80$  good agreement and  $>0.81$  very good agreement.

The overall diagnostic accuracy of each image set was determined by comparing against the gold standard tests of histopathology or follow-up imaging. The area under each reader-specific ROC curve ( $A_z$ ) was calculated and pairwise comparison made between and within readers using the variance z-test.

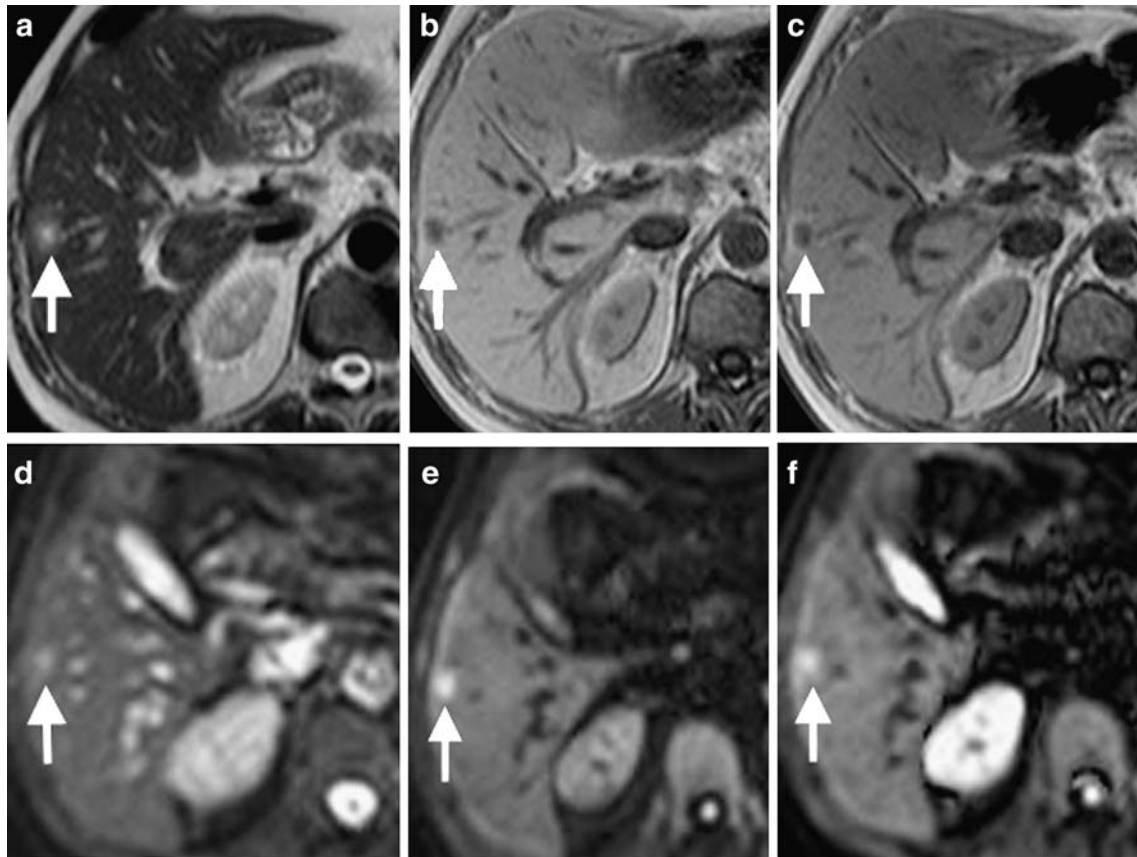


**Fig. 1** Appearance of colorectal metastasis at MnDPDP MR imaging and DWI. (a) T2-weighted MR shows a mildly hyperintense lesion in right lobe of liver, which is (b) hypointense on the 20-min post-MnDPDP enhanced T1-weighted image. (c) The lesions show rim

enhancement at T1-weighted imaging 24 h after contrast administration. (d–f) DWI images of  $b=0, 150$  and  $500 \text{ s/mm}^2$  show high signal intensity restricted diffusion within the metastasis

The sensitivity and specificity on a lesion-by-lesion basis (including the 95% confidence intervals) for each image set were calculated for each observer. Lesions scored 4 and 5 were considered malignant, and lesions with scores of 1–3 (which included those not seen) were deemed benign. The averaged sensitivity and specificity of the two observers for each image set was calculated. Comparison of the averaged sensitivity and specificity for each image set was made using the chi-square test. For all statistical analyses, a p-value of <0.05 was taken to be statistically significant.

**Results**

One hundred thirty-three lesions were documented on histopathology and follow-up imaging in 33 patients, of which 83 were metastases and 50 were benign (52 cysts, 1 haemangioma). A significant number of cysts (n=25) were identified in three patients with multiple liver cysts. Confirmation by pathology was obtained in 40/83 (48%) metastases and 16/50 (32%) benign lesions. Another 43 lesions showed at least 20% increase in lesion size at follow-up imaging and were deemed to represent metastases.

A mean number of 4.3 (range 1–15) lesions were found in each patient, with a mean size of 19.6 mm (range 5–95 mm). Forty per cent of lesions were located in the left lobe with the majority 60% in the right lobe.

**Interobserver agreement**

There was good interobserver agreement in classifying the focal liver lesions into categories 1–5 and ‘not seen’ using all the imaging combinations. The results for interobserver agreement for MnDPDP image set (kappa=0.66; 95% CI: 0.55–0.77) and DWI image set (kappa=0.68; 95% CI: 0.57–0.79) were as shown in Tables 1 and 2. There was

**Table 1** Interobserver agreement in the scoring of focal liver lesions on MnDPDP MR imaging combined with unenhanced T1- and T2-weighted MR imaging

Observer 2	Observer 1						‘Not seen’
	1	2	3	4	5		
1	37	1	0	0	0	2	40
2	2	2	0	1	0	1	6
3	0	1	0	0	1	1	3
4	1	0	0	1	2	0	4
5	2	0	0	2	59	2	65
NS	3	0	0	2	5	5	15
	45	6	3	10	73	11	133

Kappa=0.66 (95% CI: 0.55–0.77)

**Table 2** Interobserver agreement in the scoring of focal liver lesions on DWI combined with unenhanced T1- and T2-weighted MR imaging

Observer 2	Observer 1						‘Not seen’
	1	2	3	4	5		
1	38	0	1	0	0	2	41
2	0	0	0	0	0	0	0
3	0	0	0	0	0	0	0
4	0	0	0	0	0	0	0
5	2	0	1	0	58	14	75
NS	4	0	0	0	2	11	17
	44	0	2	0	60	27	133

Kappa=0.68 (95% CI: 0.57–0.79)

also good interobserver agreement in using the combined MnDPDP and DWI image set (kappa=0.78; 95% CI: 0.67–0.88).

**Diagnostic accuracy**

The ROC curves for the two observers are presented in Fig. 2.

(1) *Comparison within observers*

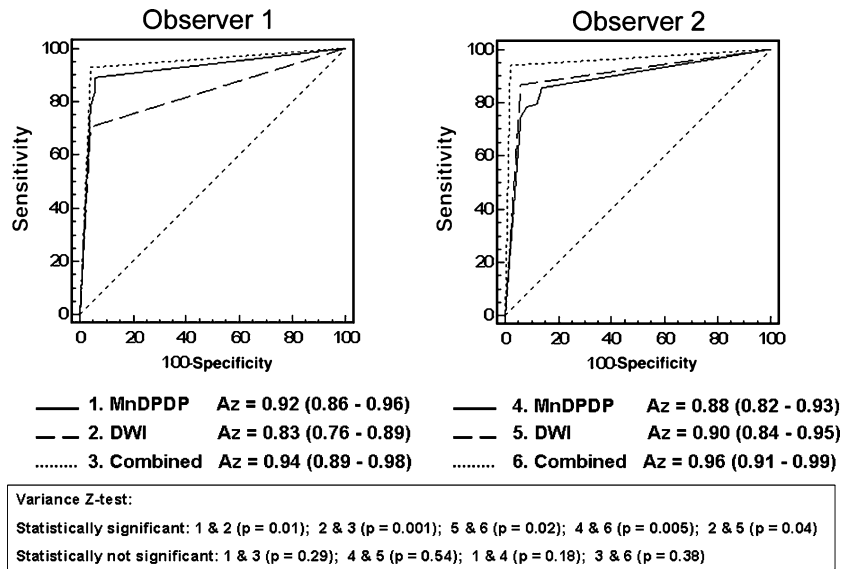
For observer 1, the diagnostic accuracy of MnDPDP image set (Az=0.92; 95% CI: 0.86–0.96) was significantly better than DWI image set (Az=0.83; 95% CI: 0.76–0.89) (p=0.01). However, for observer 2, there was no significant difference between MnDPDP image set (Az=0.88, 95% CI: 0.82–0.93) and DWI image set (Az=0.90, 95% CI: 0.84–0.95) (p=0.54). However, using the combined MnDPDP and DWI image set resulted in the highest Az in both observers (observer 1 Az=0.94; 95% CI: 0.89–0.98 and observer 2 Az=0.96; 95% CI: 0.91–0.99). For observer 1, using the combined image set improved accuracy compared with the DWI image set (p=0.001), whilst for observer 2, the combined image set resulted in better diagnostic performance compared with the MnDPDP MR image set (p=0.005) or DWI image set (p=0.02).

(2) *Comparison between observers*

There was no significant difference in the diagnostic accuracy between the two observers using MnDPDP image set (p=0.18) or the combined image set (p=0.38). However, observer 2 noted 14 lesions on DWI that were not seen by observer 1 and performed better using the DWI image set compared with observer 1 (p=0.04).

By classifying lesions that were scored as 4 or 5 as malignant and those scored 1–3 (including missed lesions

**Fig. 2** Receiver operating characteristic curves for the detection of liver metastases using the MnDPDP image set, DWI image set and combined MnDPDP and DWI image set by observers 1 and 2. The areas under the curves (Az) are shown with their 95% confidence intervals. Box insert displays the results of variance z-test between Az values



categorised as NS) as benign, the sensitivity and specificity of using the three image sets for the identification of colorectal liver metastases are summarized in Table 3. There was no significant difference in the averaged sensitivity of lesion detection using MnDPDP or DWI image sets. Using the combined image set improved the averaged sensitivity of lesion detection compared with the DWI image set (p=0.01, chi square test) and a trend towards improved sensitivity of lesion detection compared with the MnDPDP image set (p=0.06, chi square test). There was no difference in the averaged specificity of lesion detection using any of the three image sets (p>0.5, chi square test).

**Missed or misclassified metastases at MnDPDP MR imaging and DWI**

The number of metastases that were missed or misclassified using the MnDPDP set and DWI image set were compared for each observer in Table 4.

For observer 1, 13/83 metastases were missed or misclassified using the MnDPDP image set. Of these,

5/13 were missed. On review, all were ≤1 cm in diameter, 3/5 were adjacent to blood vessels (Fig. 3) and 2/5 near the edge of liver. Eight of 13 were misclassified, of which 7/8 did not show typical enhancement at imaging, 6/8 were ≤1 cm diameter, 2/8 near the edge of liver and 4/8 adjacent to blood vessels. Twenty-five of 83 metastases were missed or misclassified using the DWI image set. Of these, 21/25 were missed, but on review, 17/21 could be identified on careful review of all images, 16/21 were adjacent to blood vessels (Fig. 4), 15/21 were ≤1 cm in diameter and 10/21 were associated with DWI artefacts (Fig. 4). Four of 25 were misclassified because of DWI artefacts.

For observer 2, 18/83 metastases were missed or misclassified using the MnDPDP image set. Of these, 9/18 were missed, but retrospective review revealed all were ≤1 cm, 7/9 adjacent to blood vessels and 2/9 near the liver edge. Nine of 18 were misclassified, of which 6/9 did not show typical enhancement features, 7/9 were ≤1 cm, 4/9 were adjacent to blood vessels and 2/9 were near the liver edge. Eleven of 83 metastases were missed or misclassified using the DWI image set. Of these, 2/11 were missed because of artefacts. Of the 9/11 misclassified lesions, 5/9

**Table 3** Diagnostic sensitivity and specificity of individual observers and the average in detecting colorectal liver metastasis using MnDPDP MR imaging, DWI and combination of MnDPDP MR imaging and DWI

	Observer 1		Observer 2		Average**	
	Sensitivity* % (95% CI)	Specificity* % (95% CI)	Sensitivity* % (95% CI)	Specificity* % (95% CI)	Sensitivity*	Specificity*
MnDPDP MRI	84.3 (74.7–91.4)	94.0 (83.4–98.7)	78.3 (67.9–86.6)	92.0 (80.7–97.7)	81.3	93.0
DWI	69.9 (58.8–79.5)	96.0 (86.3–99.4)	86.7 (77.5–93.2)	94.0 (83.4–98.7)	78.3	95.0
MnDPDP + DWI	91.6 (83.4–96.5)	96.0 (86.3–99.4)	92.8 (84.9–97.3)	98.0 (89.3–99.7)	92.2	97.0

\*Score of 4 or > indicates metastasis

\*\*95% CI of averaged values not estimated

**Table 4** Comparison of the detection of malignant lesions (n=83) using MnDPDP image set and DWI image set by observers 1 and 2

Observer 1		MnDPDP image set	
		Positive	Negative
DWI image set	Positive	50	8
	Negative	20	5
Observer 2		MnDPDP image set	
DWI image set	Positive	59	13
	Negative	6	5

\*Score of 4 or 5 indicates positive test

were  $\leq 1$  cm, 6/9 were adjacent to blood vessels, but all were associated with DWI artefacts.

## Discussion

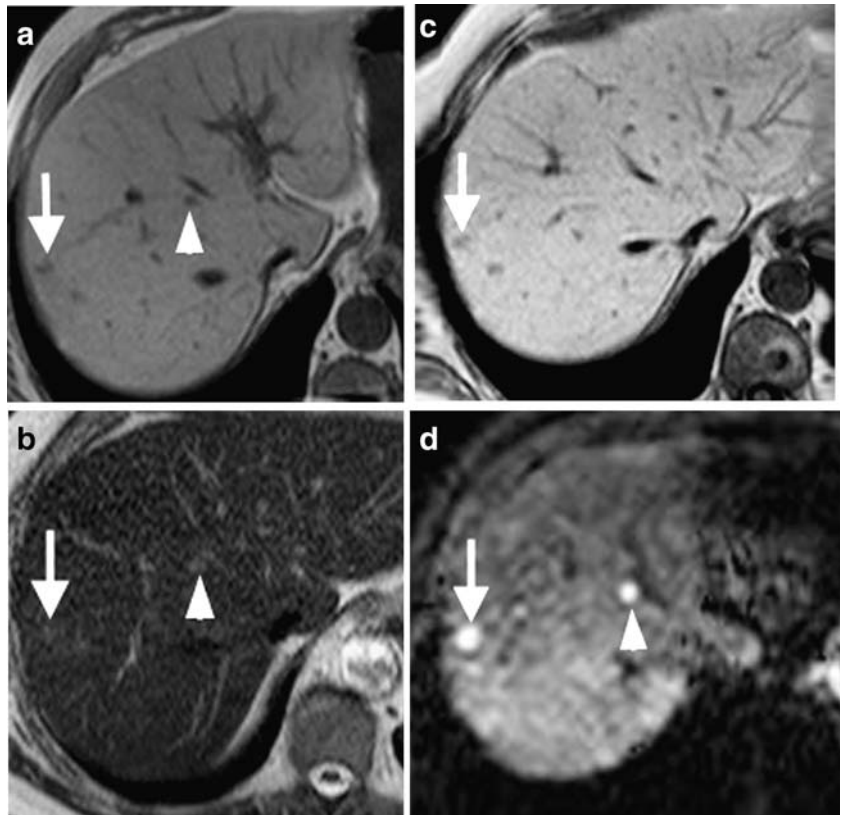
One of the key challenges to liver imaging in patients with colorectal metastases is the ability to accurately define the presence and site of liver involvement which influences treatment planning. The demonstration of extensive or unfavourable segmental involvement of liver by tumor contraindicates surgical resection. By contrast, confident demonstration of small volume metastatic disease within a

few liver segments allows accurate treatment planning by surgery or radiofrequency ablation.

By metanalysis, MR imaging was found to be more sensitive than helical CT, but less sensitive than FDG-PET imaging for detecting colorectal liver metastases [9]. However, it has been shown that MR imaging can be as sensitive as FDG-PET [10]. With the introduction of liver-specific contrast media, ferucarbotran (SPIO) enhanced MR imaging has proved to be at least as sensitive as gadolinium-chelates enhanced MR imaging [11]. More recently, a study revealed that both MnDPDP MR imaging and SPIO MR imaging have comparably high sensitivity (84–92%) for lesion detection [12]. Not surprisingly, MR imaging practices for detecting colorectal liver metastases vary from institution to institution, and the choice of imaging technique is likely to be influenced in part by personal experience and preferences.

In this study, we have demonstrated the improved diagnostic accuracy of a combined MnDPDP MR imaging and DWI approach for the detection of liver metastases. MnDPDP MR imaging on its own has been shown to be a useful technique for liver metastases [7, 13–15], and performing studies immediately and at 24 h after intravenous MnDPDP contrast infusion is useful for lesion detection [6, 16]. In our study, using the MnDPDP image set resulted in high diagnostic accuracy ( $A_z=0.92$  and  $A_z=0.88$ ), similar to those reported ( $A_z=0.91$ ) in a recent study [12].

**Fig. 3** Missed lesion at MnDPDP MR imaging. (a) Unenhanced T1-weighted, (b) T2-weighted, (c) 20-min post MnDPDP contrast T1-weighted and (d) DWI  $b=500$  s/mm<sup>2</sup> images. The unenhanced T1- and T2-weighted images showed a small lesion (white arrow) in the periphery of the right lobe of the liver, which appeared hypointense at MnDPDP MR imaging, consistent with a metastasis. However, a further small metastasis adjacent to the middle hepatic vein was missed (white arrowhead). Note non-visualization of the lesion on MnDPDP MR imaging. The lesion was clearly seen at DWI (white arrowhead)



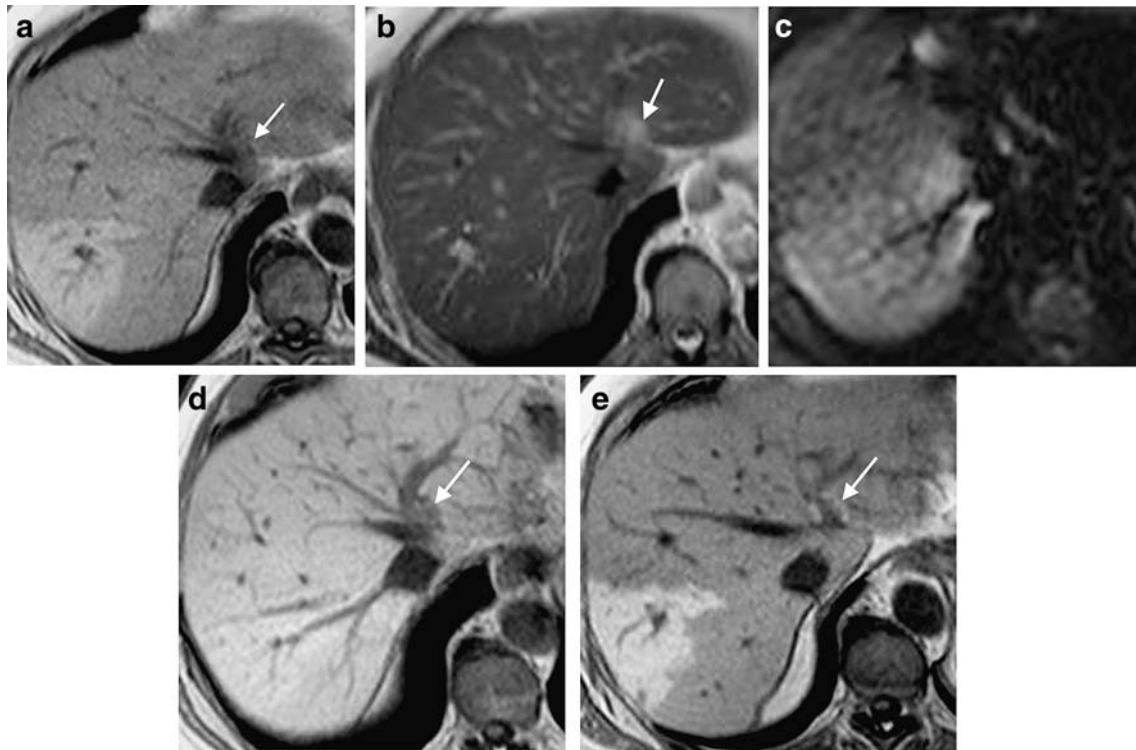


**Fig. 4** Missed metastasis at DWI. (a) Unenhanced T1-weighted, (b) T2-weighted and (c) DWI  $b=500 \text{ s/mm}^2$  images. On the T1-weighted image, there was segmental hyperintensity in the right lobe due to focal fatty infiltration. A metastasis adjacent to the left hepatic vein (arrow) was missed because of its close proximity to the

vessel and was not visualized at DWI because of cardiac motion artefacts over the left lobe of liver. The lesion was revealed as a low signal intensity lesion (arrow) on the (d) MnDPDP-enhanced T1-weighted imaging at 20 min, which showed (e) rim enhancement (arrow) at 24 h after MnDPDP contrast

DWI has not been used routinely for liver imaging as its implementation in the abdomen is challenging. Technological advancements such as parallel imaging, improvements in receiver coils and gradients technology, as well as echo-planar imaging together, enable high quality DWI images of the liver to be obtained using single-shot breath-hold acquisitions [17]. Nasu et al. [8] showed that by applying such a technique, DWI ( $Az=0.90$ ) was superior to SPIO-enhanced MR imaging ( $Az=0.81$ ) for detecting liver metastases on a per-lesion basis averaged across three observers. Recently, it has been shown that DWI performed after the administration SPIO can also improve lesion detection by suppression of the liver signal [18].

In our study, the diagnostic accuracy using the DWI image set was good, but was better for observer 2 compared with observer 1 ( $Az=0.90$  versus  $Az=0.83$ ,  $p=0.04$ ). This difference was most likely related to observer experience, which has been shown to affect diagnostic performance. Observer 2 was more experienced in reviewing DWI images compared with observer 1. DWI images are sensitive to motion, susceptibility and ghosting artefacts, which can obscure lesions and confound interpretation. Thus, experience and patience are needed to build confidence in recognizing abnormalities when reviewing large numbers of DWI images. Because artifacts

from one directional image may propagate into the calculated trace or index image, lesions can be missed if only the trace images are reviewed.

Our study also revealed that missed or misclassified lesions at MnDPDP MR imaging and DWI were often  $\leq 1 \text{ cm}$  in size and found adjacent to intra-hepatic blood vessels. At MnDPDP MR imaging, both blood vessels and metastases appear hypointense on T1-weighted imaging, and small metastases may be mistaken for blood vessels. Hence, the radiologist should be careful in surveying areas adjacent to blood vessels when applying this technique. Using breath-hold DWI, artefacts arising from cardiac motion or susceptibility effects can obscure lesions, particularly over the left lobe of the liver [8]. When this occurs, small lesions adjacent to blood vessels are also more easily overlooked on the unenhanced T1- and T2-weighted images. Acquisition techniques that increase signal-to-noise and decrease artefacts (e.g. free breathing and navigator-controlled acquisition) can improve the quality of DWI and should be investigated in future studies.

There were several limitations to our study. Firstly, the study was conducted in a highly selected population of patients with colorectal cancer with a high pre-test probability of detecting metastases. Thus, it is unclear as to what degree the current findings can be generalized to

the wider population or to patients with other types of cancers. Secondly, the DWI and MnDPDP MR images were assessed in combination with the unenhanced T1-/T2-weighted images. As such, the diagnostic effects of DWI and MnDPDP MR imaging alone could not be isolated. However, the image sets reflect clinical practice where several imaging sequences are usually combined for diagnostic evaluation. Thirdly, it was not possible fully to test the ability of DWI to characterize lesions detected since almost all benign lesions in our study group were cysts. This may have introduced bias in the results. Fourthly, we only evaluated the native DWI images and did not review the ADC maps in this study. However, ADC maps are usually noisier, and it is doubtful that reviewing these

would improve lesion detection, although it is possible that ADC maps may help in lesion characterization in future studies.

## Conclusions

In patients with colorectal hepatic metastases, the combination of MnDPDP MR imaging and DWI improved the diagnostic accuracy and can increase sensitivity without loss in specificity, compared with either technique alone.

**Acknowledgements** This research was supported by Cancer Research UK Grant C1060/A808.

## References

1. Yamada H, Katoh H, Kondo S, Okushiba S, Morikawa T (2001) Repeat hepatectomy for recurrent hepatic metastases from colorectal cancer. *Hepatogastroenterology* 48:828–830
2. Bolton JS, Fuhrman GM (2000) Survival after resection of multiple bilobar hepatic metastases from colorectal carcinoma. *Ann Surg* 231:743–751
3. Brand MI, Saclarides TJ, Dobson HD, Millikan KW (2000) Liver resection for colorectal cancer: liver metastases in the aged. *Am Surg* 66:412–415; discussion 415–416
4. Scheele J, Stang R, Altendorf-Hofmann A, Paul M (1995) Resection of colorectal liver metastases. *World J Surg* 19:59–71
5. Masi G, Cupini S, Marcucci L, Cerri E, Loupakis F, Allegrini G, Brunetti IM, Pfanner E, Viti M, Goletti O, Filipponi F, Falcone A (2006) Treatment with 5-fluorouracil/folinic acid, oxaloplatin, and irinotecan enables surgical resection of metastases in patients with initially unresectable metastatic colorectal cancer. *Ann Surg Oncol* 13:58–65
6. Koh DM, Brown G, Meer Z, Norman AR, Husband JE (2007) Diagnostic accuracy of rim and segmental MRI enhancement of colorectal hepatic metastasis after administration of mangafodipir trisodium. *AJR Am J Roentgenol* 188:W154–161
7. Bartolozzi C, Donati F, Cioni D et al (2004) Detection of colorectal liver metastases: a prospective multicenter trial comparing unenhanced MRI, MnDPDP-enhanced MRI, and spiral CT. *Eur Radiol* 14:14–20
8. Nasu K, Kuroki Y, Nawano S et al (2006) Hepatic metastases: diffusion-weighted sensitivity-encoding versus SPIO-enhanced MR imaging. *Radiology* 239:122–130
9. Bipat S, van Leeuwen MS, Comans EF et al (2005) Colorectal liver metastases: CT, MR imaging, and PET for diagnosis-meta-analysis. *Radiology* 237:123–131
10. Yang M, Martin DR, Karabulut N, Frick MP (2003) Comparison of MR and PET imaging for the evaluation of liver metastases. *J Magn Reson Imaging* 17:343–349
11. Ward J, Robinson PJ, Guthrie JA et al (2005) Liver metastases in candidates for hepatic resection: comparison of helical CT and gadolinium- and SPIO-enhanced MR imaging. *Radiology* 237:170–180
12. Choi JY, Kim MJ, Kim JH et al (2006) Detection of hepatic metastasis: manganese- and ferucarbotran-enhanced MR imaging. *Eur J Radiol* 60:84–90
13. Beziat C, Pilleul F, Yzebe D, Lombard-Bohas C, Mercier C, Valette PJ (2004) [Detection of liver metastases in colorectal cancer on chemotherapy. Comparative study between MRI with teslascan and computed tomography with intravenous contrast media]. *J Radiol* 85:307–311
14. Grimm J, Muller-Hulsbeck S, Blume J, Biederer J, Heller M (2001) [Comparison of biphasic spiral CT and MnDPDP-enhanced MRI in the detection and characterization of liver lesions]. *Rofo* 173:266–272
15. Kim KW, Kim AY, Kim TK et al (2004) Small (<or= 2 cm) hepatic lesions in colorectal cancer patients: detection and characterization on mangafodipir trisodium-enhanced MRI. *AJR Am J Roentgenol* 182:1233–1240
16. Kane PA, Ayton V, Walters HL et al (1997) MnDPDP-enhanced MR imaging of the liver. Correlation with surgical findings. *Acta Radiol* 38:650–654
17. Koh DM, Collins DJ (2007) Diffusion-weighted MRI in the body: applications and challenges in oncology. *AJR Am J Roentgenol* 188:1622–1635
18. Kiryu S, Watanabe M, Kabasawa H, Akahane M, Aoki S, Ohtomo K (2006) Evaluation of super paramagnetic iron oxide-enhanced diffusion-weighted PROPELLER T2-fast spin echo magnetic resonance imaging: Preliminary experience. *J Comput Assist Tomogr* 30:197–200